nature neuroscience

'Silent' mitral cells dominate odor responses in the olfactory bulb of awake mice

Mihaly Kollo[1,2], Anja Schmaltz[1,3], Mostafa Abdelhamid[1,3], Izumi Fukunaga[1,2] & Andreas T Schaefer[1–4]

How wakefulness shapes neural activity is a topic of intense discussion. In the awake olfactory bulb, high activity with weak sensory-evoked responses has been reported in mitral/tufted cells (M/TCs). Using blind whole-cell recordings, we found 33% of M/TCs to be 'silent', yet still show strong sensory responses, with weak or inhibitory responses in 'active' neurons. Thus, a previously missed M/TC subpopulation can exert powerful influence over the olfactory bulb.

Sensory processing is thought to be markedly influenced by behavioral state. Substantial amounts of data have been obtained from anesthetized preparations, yet recent results from awake animals suggest substantially altered network activity[1–5]. In the olfactory system, studies using extracellular local field potential and single-unit recordings[4–9] or calcium imaging[2,10,11] have reported substantially increased baseline activity of M/TCs in the awake animal (but see ref. 3) and only weak, transient or inhibitory odor-evoked responses (but see ref. 12). All currently available techniques, however, allow recording from only a fraction of neurons in mammalian neuronal networks[13]. Thus, the sampling characteristics and internal error sources of different recording techniques have to be taken into consideration to gain global insight into network dynamics[14,15].

We used blind whole-cell recordings to measure the activity *in vivo* of 125 olfactory bulb neurons in the awake, alert state (**Supplementary Figs. 1** and **2**) and 179 neurons in the anesthetized state. Recordings from M/TCs revealed highly heterogeneous baseline states (**Fig. 1**). The resting membrane potentials of M/TCs showed significantly larger dispersion in awake animals ($P = 0.020$, modified robust Brown-Forsythe Levene test; $IQR_{awake} = 6.32$ mV, $IQR_{anesthetized} = 4.83$ mV; **Fig. 1c**,**f**,**g**), with more neurons at relatively hyperpolarized or relatively depolarized membrane potentials (**Fig. 1g**). Consequently, in awake animals, a larger proportion of cells were highly active (firing rate > 10 Hz in 15% of M/TCs versus 5% in anesthetized; **Fig. 1h**), yet both in the awake and anesthetized state, one-third of the neurons showed very low baseline firing rates (<0.1 Hz). Thus, consistent with previous studies[3,8,12], we found that, under baseline conditions, there are substantially more highly active cells in the awake than in the anesthetized preparation. Blind whole-cell recordings, however, also revealed a substantial silent subpopulation of M/TCs that rarely or never spontaneously discharge action potentials in the awake animal, but are otherwise indistinguishable from more active cells (**Supplementary Fig. 2**).

We next characterized the evoked response profiles of neurons to short (1–2.5 s) odor pulses presented passively to the animals or during an odor discrimination task (**Supplementary Fig. 1**). The activity of M/TCs was modulated in a highly diverse manner by odor stimulation in awake mice (**Fig. 2**). The occurrence of inhibitory and excitatory responses was balanced (54% excitatory, 46% inhibitory, **Fig. 2b**), but, in some neurons, we observed particularly strong phasic depolarizing reactions to odorants (**Fig. 2a**). Notably, M/TCs with low spontaneous activity responded predominantly with depolarization and increased rate, whereas M/TCs with high baseline spiking activity (consistent with previous observations[3,8]) responded mostly with weak excitation or hyperpolarization ($P < 0.001$, Mann-Whitney U test, $n = 52$ and 50 significant odor responses; **Fig. 2c** and **Supplementary Fig. 3**). Similarly, response profiles of more depolarized cells showed a preference for inhibitory or only weakly excitatory responses ($\rho = -0.39$, $P < 0.001$, Spearman's rank correlation; **Fig. 2d**), whereas hyperpolarized cells regularly responded to odorants with strong, phasic depolarization. A weaker, but similar, relationship was found under anesthesia (**Supplementary Figs. 3** and **4**). Conversely, in control trials without odors, no significant correlation was found between recent baseline membrane potential and response ($\rho = -0.0084$, $P = 0.87$) or recent firing rate and response ($\rho = -0.027$, $P = 0.61$), confirming that the association in odor trials does not arise from regression to mean that could derive from, for example, random fluctuations in the baseline of M/TCs.

Most unit recordings report an overall higher baseline activity[4,8,12] (but see ref. 3) and weaker excitatory responses in awake compared with anesthetized preparations[3,8] (but see ref. 12), which we similarly observed in the more active cells measured with whole-cell recordings (**Supplementary Table 1**). In addition, multiple studies reported transient[3–5] and context-dependent responses[7,16,17] in M/TCs. We found that the gross time courses of responses differed somewhat between the anesthetized and awake states. Phasic responses during odor presentation were closely matched between awake and anesthetized animals (**Fig. 2** and **Supplementary Fig. 3**). Long-lasting responses that well exceeded the time of odor presentation[18], however, were much more common in the anesthetized state (**Supplementary Fig. 5**; also see ref. 11).

We found that, contrary to what has been suggested previously, the transition from the anesthetized to the awake state is not characterized by an overall increase in activity and a reduction of responses to primary sensory stimuli. Instead, the variability of M/TC activity is increased. This in turn creates a population of highly active, weakly odor-responding cells; there was, however, a continuum of firing rates,

[1]Behavioural Neurophysiology, Max Planck Institute for Medical Research, Heidelberg, Germany. [2]Division of Neurophysiology, MRC National Institute for Medical Research, London, UK. [3]Department of Anatomy and Cell Biology, Faculty of Medicine, University of Heidelberg, Heidelberg, Germany. [4]Department of Neuroscience, Physiology and Pharmacology, University College London, London, UK. Correspondence should be addressed to M.K. (mihaly.kollo@mpimf-heidelberg.mpg.de) or A.T.S. (andreas.schaefer@mpimf-heidelberg.mpg.de).

Received 12 May; accepted 26 June; published online 27 July 2014; doi:10.1038/nn.3768

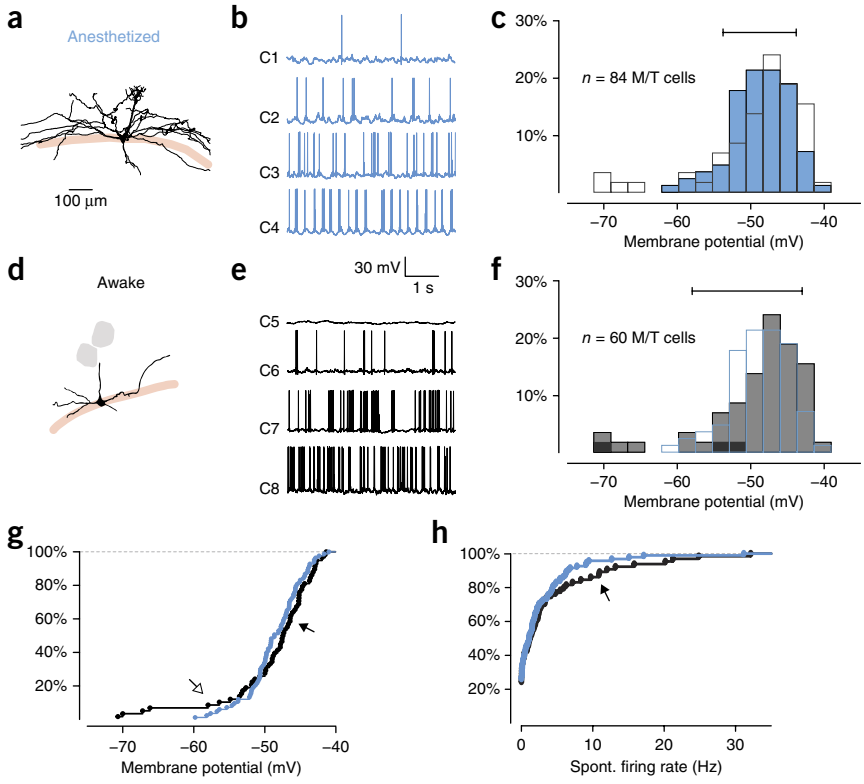

Figure 1 Baseline states of M/TCs in awake and anesthetized mice. (**a**–**f**) Patch-clamp recordings from M/TCs of anesthetized (**a**–**c**) and awake mice (**d**–**f**). (**a**,**d**) Representative morphological reconstructions. (**b**,**e**) Four example M/TC recordings of baseline activity in each the awake (**e**, black) and the anesthetized (**b**, blue) preparation. (**c**,**f**) Distribution of baseline membrane potentials in M/TCs. Horizontal bars indicate the 10–90 percentile range. Dark gray bars in (**f**) represent recordings while the animal was performing an odor discrimination task (**Supplementary Fig. 1**). Hollow bars indicate the awake (**c**, black) and anesthetized (**f**, blue) data for direct comparison. (**g**) Cumulative distribution of baseline membrane potential in M/TCs in awake (black, $n = 60$ M/TCs from 45 animals) and anesthetized (blue, $n = 84$ M/TCs from 51 animals) animals. Arrows indicate the increased number of both relatively hyperpolarized (open arrow) and relatively depolarized cells (black arrow) in recordings from awake compared with anesthetized mice. (**h**) Distribution of M/TC firing rates of the same populations of cells as in **g** recorded in anesthetized (blue) or awake (black) mice. The black arrow indicates the significantly larger population of M/TCs in the awake animal with high baseline firing rate (firing rate > 10 Hz in 9 of 60 M/TCs in awake versus 4 of 84 M/TCs in anesthetized).

including a substantial population of cells in the awake state that is virtually silent at baseline conditions, but can vigorously respond to odor presentation. Although whole-cell recordings themselves might suffer from specific biases and technical drawbacks, they can record from cells that show little or no spiking under resting conditions—a population of cells that has not been studied intensely with recording techniques predominantly relying on action potentials for cell detection. One aspect of the observed heterogeneity in both the baseline activity levels and odor responses of M/TCs is how the divergent principal cells might influence postsynaptic local interneurons (INs) and, consequently, the transformation of odor representations in the olfactory bulb, including proposed circuit functions such as contrast enhancement or pattern completion. Our results indicate that M/TCs with high baseline firing rates would be less able to exert a strong excitatory effect onto and therefore recruit INs. First, such neurons rarely respond with depolarization to odorants, which would be necessary to evoke increased transmitter release. Moreover, excitatory synapses between M/TCs and INs express short-term depression[19,20]. Consequently, synapses from highly active M/TCs will be depressed compared with synapses from low firing rate M/TCs (**Supplementary Figs. 6–8**). Downstream targets in turn might be engaged preferentially by different populations of M/TCs through largely facilitating synapses. Mechanistically, differing electrical driving force and feedback in the glomerulus or onto olfactory sensory neuron terminals might contribute to the activity dependence of evoked responses. Recordings in behaving, awake animals have shown that M/TC activity is highly dynamic on longer time scales[2] and is influenced by inputs from higher order brain regions[7,9], suggesting that the principal source of variability of neuronal activity in the olfactory bulb in awake animals is strong top-down modulation. It remains to be shown how the different behavioral states may influence the pattern of M/TC baseline activity.

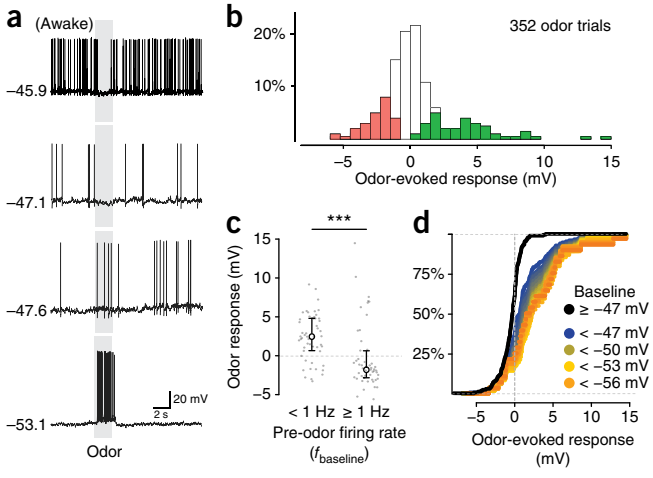

Figure 2 Odor-evoked responses in M/TCs in awake mice are predicted by baseline activity. (**a**) Example traces of odor-evoked responses in four M/TCs recorded in awake mice. The respective average baseline membrane potential is indicated to the left of each trace (in mV). (**b**) Histogram of odor response amplitudes in M/TCs ($n = 36$ M/TCs from 36 animals, $n = 352$ odor responses). Significant ($P < 0.05$, see Online Methods) responses are displayed in green ($n = 55$ odor responses) and red ($n = 47$) for depolarizing and hyperpolarizing responses, respectively. (**c**) Relationship between recent firing behavior and odor-evoked responses (mean and 25th and 75th percentile, $n = 52$ odor-cell pairs from 15 M/TCs from 15 animals for $f_{baseline} < 1$ Hz and $n = 50$ from 13 M/TCs from 13 animals for $f_{baseline} \geq 1$ Hz). ***$P < 0.001$, Mann-Whitney U-test. (**d**) Cumulative distribution curves displaying the dependence of the odor response profiles of M/TCs on recent membrane potential (<–56 mV, $n = 26$ odor-cell pairs; <–53 mV, $n = 38$; <–50 mV, $n = 46$; <–47 mV, $n = 53$; ≥–47 mV, $n = 49$). The most hyperpolarized cells (orange trace) responded preferentially with strong excitation, whereas depolarized cells (black trace) mainly showed inhibition.

METHODS

Methods and any associated references are available in the online version of the paper.

Note: Any Supplementary Information and Source Data files are available in the online version of the paper.

ACKNOWLEDGMENTS

We thank M. Kaiser, E. Stier, S. Bellanca, P. Hasel and M. Karageorgi for technical assistance, N. Neef and M. Lukat for building the treadmill and headplates, and R. Jordan for help with behavioral experiments. We also thank D. Gire, R. Haddad, L. Kay and D. Rinberg for discussion, and T. Margrie, Z. Nusser and D. Burdakov for comments on the manuscript. This work was supported by the Excellence Cluster Cell Networks (postdoctoral fellowship to M.K.), the Max Planck Society, DFG (SPP1392), the Medical Research Council (MC_UP_1202/5), and the Alexander von Humboldt foundation (postdoctoral fellowship to I.F.). A.T.S. is a member of the Interdisciplinary Center for Neuroscience and the Bernstein-Center.

AUTHOR CONTRIBUTIONS

M.K. and A.T.S. designed and conceived all of the experiments. A.S. designed the headplate and the treadmill. M.K. performed the awake recordings and the computational analyses. M.K. and I.F. carried out the anesthetized experiments. M.A. performed the behavioral experiments. M.K. and A.T.S. analyzed and interpreted the data and modeling results. M.K. and A.T.S. wrote the article with contributions from all authors.

COMPETING FINANCIAL INTERESTS

The authors declare no competing financial interests.

1. Haider, B., Häusser, M. & Carandini, M. *Nature* **493**, 97–100 (2013).
2. Kato, H.K., Chu, M.W., Isaacson, J.S. & Komiyama, T. *Neuron* **76**, 962–975 (2012).
3. Gschwend, O., Beroud, J. & Carleton, A. *PLoS ONE* **7**, e30155 (2012).
4. Shusterman, R., Smear, M.C., Koulakov, A. & Rinberg, D. *Nat. Neurosci.* **14**, 1039–1044 (2011).
5. Cury, K.M. & Uchida, N. *Neuron* **68**, 570–585 (2010).
6. Fuentes, R.A., Aguilar, M.I., Aylwin, M.L. & Maldonado, P.E. *J. Neurophysiol.* **100**, 422–430 (2008).
7. Kay, L.M. & Laurent, G. *Nat. Neurosci.* **2**, 1003–1009 (1999).
8. Rinberg, D., Koulakov, A. & Gelperin, A. *J. Neurosci.* **26**, 8857–8865 (2006).
9. Doucette, W. & Restrepo, D. *PLoS Biol.* **6**, e258 (2008).
10. Blauvelt, D.G., Sato, T.F., Wienisch, M., Knöpfel, T. & Murthy, V.N. *Front. Neural Circuits* **7**, 46 (2013).
11. Wachowiak, M. *et al. J. Neurosci.* **33**, 5285–5300 (2013).
12. Davison, I.G. & Katz, L.C. *J. Neurosci.* **27**, 2091–2101 (2007).
13. Shoham, S., O'Connor, D.H. & Segev, R. *J. Comp. Physiol. A Neuroethol. Sens. Neural Behav. Physiol.* **192**, 777–784 (2006).
14. Margrie, T.W., Brecht, M. & Sakmann, B. *Pflugers Arch.* **444**, 491–498 (2002).
15. Wohrer, A., Humphries, M.D. & Machens, C.K. *Prog. Neurobiol.* **103**, 156–193 (2013).
16. Pager, J. *Brain Res.* **289**, 87–98 (1983).
17. Bhalla, U.S. & Bower, J.M. *J. Comput. Neurosci.* **4**, 221–256 (1997).
18. Matsumoto, H., Kashiwadani, H., Nagao, H., Aiba, A. & Mori, K. *J. Neurophysiol.* **101**, 1890–1900 (2009).
19. Balu, R., Pressler, R.T. & Strowbridge, B.W. *J. Neurosci.* **27**, 5621–5632 (2007).
20. Dietz, S.B. & Murthy, V.N. *J. Physiol.* (*Lond.*) **569**, 475–488 (2005).

ONLINE METHODS

Animals. C57BL/6J mice aged 4–7 weeks were used in both anesthetized and awake recordings. Animals from both sexes were used randomly (49.5%/50.5%). Before experiments, up to five mice were co-housed in a cage. From the start of the experiment, animals were housed in separate cages. Animals were kept in normal light/dark cycle and behavioral experiments were performed during the night hours. All animal experiments were performed in accordance with the German Animal Welfare Act.

Surgery. Mice were anesthetized using ketamine (100 mg per kg of body weight) and xylazine (20 mg per kg for induction, 10 mg per kg for maintenance) administered intraperitoneally and supplemented as required. Body temperature was maintained at 37.0 °C with a feedback-regulated heating pad (FHC). A custom-made steel or PEEK headplate was fixed to the parietal bone plates with cyanoacrylate and dental cement. During surgery, meloxicam (2.5 mg per kg) was injected intraperitoneally for post-operative analgesia. Animals were allowed to recover for 2–7 d. On the day of the recording, under brief isoflurane anesthesia (1.5%, vol/vol, analgesia was provided by 2.5 mg per kg intraperitoneal meloxicam and local application of 1% lidocaine, wt/vol), a small (0.4–0.8 mm) craniotomy was drilled above the olfactory bulb. For anesthetized recordings, ketamine and xylazine was administered intraperitoneally. After removal of the dura, the craniotomy was covered by a layer of low melting–point agarose (0.5–1 mm). The chamber surrounding the craniotomy was filled with Ringer solution (135 mM NaCl, 5.4 mM KCl, 5 mM HEPES, 1 mM $MgCl_2$, 1.8 mM $CaCl_2$, pH 7.2, 285 mOsm kg^{-1}) to prevent desiccation. For awake recordings, animals were head-fixed on a linear treadmill as described previously[21] to minimize stress. Following awakening after surgery, the animals were allowed to recover for at least 30 min before electrophysiological recordings commenced[22]. No overt stress responses were observed and all animals readily accepted food and licked for rewards well before that time. Consistent with previous studies[2], no differences were found if animals were acclimatized to the head-fixation over the course of several days (**Supplementary Figs. 1** and **3**) and data was thus pooled.

Odor delivery. Odors (anisaldehyde, cinnamaldehyde, cyclohexanol, estragol, eugenol, isoamyl acetate, methyl salycilate, 1-octanol, phenyl-ethanol, salycilate and vanillin) were presented using a custom-made airflow dilution olfactometer with electronic dilution control to result in a final concentration of 40 ppm (range 0.1–520 ppm) on average. Odors were presented individually with a minimal inter-trial interval of 10 s. No intrinsic aversive or attractive behavioral reaction to the odors was observed and all odors were readily learned as S+ as well as S– stimuli. To achieve minimal contamination and a reproducible stimulus shape, the olfactometer was washed by a strong stream of clean air between odor trials, while constant air flow to the animal was established by a final valve at the odor port. A photo ionization detector (miniPID, Aurora Scientific) was used regularly to determine the time course of odor presentation and ascertain the absence of contamination.

Electrophysiology. Whole-cell recordings were made as described previously[14], with borosilicate glass capillaries pulled to 5–10-MΩ resistance when filled with solution containing 130 mM $KMeSO_4$, 10 mM HEPES, 7 mM KCl, 2 mM ATP-Na, 2 mM ATP-Mg, 0.5 mM GTP, 0.05 mM EGTA, 10 mM biocytin and 10 mM Alexa594. pH and osmolality were adjusted to 7.3 and 275–280 mOsm kg^{-1}, respectively. Signals were amplified using a Multiclamp 700B amplifier (Molecular Devices) and digitized by a Micro 1401 (Cambridge Electronic Design) at 30 kHz. Drift in membrane potential between the first 5 s and first 1 min was −1.07 ± 2.75 mV (mean ± s.d.), and 0.78 ± 0.82 mV between the first 1 min and the first 10 min. Recording lengths from M/TCs in awake animals ranged from 0.5–35 min, with a median of 11.34 min.

Identification of cell classes. For postmortem morphological identification of neurons (22 of 304 recorded neurons were recovered sufficiently well to allow for unequivocal identification as interneuron or principal neuron, M/TC). A subset of these has been described previously[21], including the morphology shown in **Figure 1a**. Alexa 594–filled cells were imaged using a custom-built two-photon microscope. Subsequently, mice were perfused following the acute electrophysiological experiment with cold phosphate-buffered saline with 137 mM NaCl, 2.8 mM KCl, 1.5 mM KH_2PO_4, 8.1 mM Na_2HPO_4, pH 7.4, osmolality (286 mOsm kg^{-1}) followed by 4% formaldehyde (wt/vol) solution in phosphate-buffered saline. Fixed olfactory bulbs were cut with a vibratome (Microm) and stained with avidin-biotinylated peroxidase (ABC kit, Vector Labs) and the diaminobenzidine reaction. Biocytin stained cells were traced using a Neurolucida system (Micro Bright Field). Mitral and tufted cells were identified by a cell body located in the mitral cell layer or the external plexiform layer, respectively, the presence of an apical dendrite progressing into the glomerular layer and lateral dendrites branching in the external plexiform layer. To separate all M/TC recordings from other cell types, we performed hierarchical clustering of the cells using three factors (**Supplementary Fig. 2**). The factors were produced by independent component analysis of the after-potential waveform (2–25 ms after the peak of the spike) of the average action potential of each cell. The after-potential was used because it is less sensitive to variability in access resistance, and distinctly characteristic to the recorded cell types. The clustering resulted in a clear and complete separation of morphologically identified M/TCs from other cell types (**Supplementary Fig. 2**). The activity of the cells showed no correlation to the three factors and accordingly active and inactive cells distributed evenly in the cluster. Notably, neither input resistance, nor other cellular parameters (except resting membrane potential) differed between silent and active cells (**Supplementary Fig. 2**).

Simulations. The time course of postsynaptic currents in granule cells has been estimated in simulation using measured M/TC spike trains and a theoretical model of synaptic depression[23,24]. Granule cell EPSC waveforms were generated by a normalized alpha function

$$\mathrm{EPSC}_0(t) = \alpha \cdot t \cdot \frac{e}{\tau_E} \cdot e^{-t/\tau_E} \quad (1)$$

where τ_E (3.6 ms) is the EPSC decay time constant and α denotes the maximal EPSC amplitude (−40 pA)[25]. During a prolonged spike train, synaptic availability decreases due to synaptic depression. At each spike, the amount of synaptic depression (D) was updated by a linear constant (d).

$$D_0 = 1 \quad (2)$$

$$D(t_{sp}^{+}) = d \cdot D(t_{sp}^{-}) \quad (3)$$

Between spikes, D recovered exponentially back toward 1 with first-order kinetics with the time constant τ_d

$$\tau d \cdot \frac{dD}{dt} = 1 - D \quad (4)$$

The resulting EPSC waveform was calculated as

$$\mathrm{EPSC}_i(t) = D(t_i) \cdot \mathrm{EPSC}_0(t - t_i) \quad (5)$$

The simulated current trace for the whole recording was calculated as the linear sum of EPSC waveforms

$$I(t) = \sum_{i=0}^{n} \mathrm{EPSC}_i(t) \quad (6)$$

Data analysis. Odor responses were calculated as activity in the first 1 s from the beginning of odor stimulation relative to the 1 s preceding the stimulus. Baseline was defined as the period 2 s to 1 s before the odor pulse. For control trials, responses were defined as the last 1 s preceding the stimulus in comparison to the time interval between 2 s and 1 s before the stimulus. Significant odor responses were defined by a bootstrapping method: 100 random 2 s regions were chosen from the baseline period, and the distribution of membrane potential difference between the first and the second half of the random windows was determined. Sensory responses with absolute membrane potential deviations exceeding the 95th percentile of the baseline fluctuation were considered significant. Voltage traces of M/TCs were normalized for offset related to the median spike threshold (−38.48 mV). Four cells in which external current was injected during the baseline period (before odorant application) were included into the cluster analysis but omitted from the analysis of membrane potential (one cell in the anesthetized state, three cells in the awake state; **Figs. 1c**,**f**,**g** and **2d**).

doi:10.1038/nn.3768

Membrane potential values were not corrected for the liquid junction potential. Data analysis was performed using Spike2 (Cambridge Electronic Design) and R 3.0.1 (http://www.R-project.org/). Sample sizes used are similar to those reported in the field and no statistical method was used to predetermine these. Animals were randomly chosen from the same age group for awake and anesthetized experiments. Male and female mice were used randomly. Odor stimuli were presented in a random order. Data collection and analysis were not performed blind to the conditions of the experiments. Due to the non-normal distribution of the data, non-parametric hypothesis tests and measures of statistical dependence were used. For comparison of odor responses in active and silent cell populations, homogeneity of variances was tested ($P = 0.542$, modified robust Brown-Forsythe Levene-type test) before the Mann-Whitney U test. All performed tests were two-sided.

A **Supplementary Methods Checklist** is available.

21. Fukunaga, I., Berning, M., Kollo, M., Schmaltz, A. & Schaefer, A.T. *Neuron* **75**, 320–329 (2012).
22. Cazakoff, B.N., Lau, B.Y.B., Crump, K.L., Demmer, H.S. & Shea, S.D. *Nat. Neurosci.* **17**, 569–576 (2014).
23. Abbott, L.F., Varela, J.A., Sen, K. & Nelson, S.B. *Science* **275**, 220–224 (1997).
24. Boegerhausen, M., Suter, P. & Liu, S.-C. *Neural Comput.* **15**, 331–348 (2003).
25. Cang, J. & Isaacson, J.S. *J. Neurosci.* **23**, 4108–4116 (2003).